Copolymer fraction effect on acid catalyzed deprotection reaction kinetics in model 193 nm photoresists [§]

Shuhui Kang[a], Vivek M. Prabhu[a], Bryan D. Vogt[a], Eric K. Lin[a], Wen-li Wu[a], Karen Turnquest[b],

[a]Polymers Division, National Institute of Standards and Technology, Gaithersburg, MD, 20899
[b]SEMATECH, 2706 Montopolis Dr, Austin, Texas 78741

ABSTRACT

A correlation between polymer molecular structure and acid catalyzed reaction kinetics is demonstrated by a photoresist copolymer with an acid-labile and a non-reactive monomer. The acid catalyzed deprotection kinetics depend significantly on the composition of the non-reactive comonomer in the polymer chain. The apparent reaction rate constant decreases monotonically with increasing non-reactive comonomer composition. The phenomena are interpreted as the reduction of diffusivity of photoacid in the polymer matrix from a hydrogen-bonding interaction with the polar group in the inert comonomer. In addition, hydrogen-bonding interactions between the photoacid and the reaction product, primarily methacrylic acid, can account for the acid loss or trapping effect observed by various researchers.

Keywords: Photolithography, photoresists, diffusion, reaction rate constants, FTIR, copolymer, photoacid, PAG

INTRODUCTION

Chemically amplified photoresists, may quickly be approaching fundamental resolution limits due to intrinsic materials and processing physics and chemistry. Current imaging technology is dependent on nanometer level control of the diffusion-reaction process of a UV sensitive photoacid generator in polymer-based photoresists containing acid-labile protection groups[1,2]. Extensive efforts have been put on understanding the mechanism and kinetics of photoresist reactions in recent years. However, most studies have focused on the physico-chemical properties of the photoacid such as the photolysis efficiency[3-9], the diffusivity[10-13] and the dissociation or acidity[14] in polymer photoresists. Fewer studies have focused on the effect of polymer photoresist and the reaction products on the reaction kinetics. The interaction between the photoacid and the polar group of photoresists or reaction products should influence the local photoacid diffusion-reaction process.

In this study, we investigate the dependence of the acid catalyzed kinetics on the copolymer composition, and UV exposure dose using Fourier transform infrared (FTIR) spectroscopy and a model 193 nm photolithography photoresist copolymer system with an acid-labile and a non-reactive monomer. A non-reactive comonomer in photoresist is sometimes used to improve the dissolution behavior of the photoresist, but the change in polymer composition could also affect the diffusion-reaction kinetics and the shape of deprotection front from the photoacid diffusion. This paper provides a systematic study of the effect of the composition of the non-reactive monomer and the reaction product on the reaction kinetics. A model of the kinetics is developed and used to interpret the FTIR data.

---

1. Materials

Poly(methyladamantyl methacrylate) (PMAdMA) and poly(methyladamantyl methacrylate-co-α-gammabutyrolactone methacrylate), containing 59 % by mol α-gammabutyrolactone methacrylate were provided by DuPont Electronic Polymers. The second copolymer containing 50 % by mol α-gammabutyrolactone methacrylate (P(MAdMA$_{50}$-co-GBLMA$_{50}$)) was supplied by AZ Electronic Materials USA Corp. The chemical structures of the three polymers are provided in Scheme 1 and their characteristics are listed in Table I. The photoacid generator triphenylsulfonium perfluorobutanesulfonate (TPS-PFBS) was supplied by Toyo Gosei. The deprotection reaction of photoresists catalyzed by photoacid is shown in scheme 2.
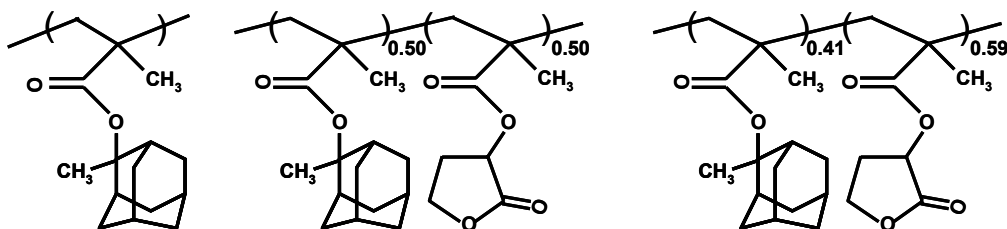
Scheme 1. Chemical structures of three photoresists used in this study;
Left: PMAdMA; middle: P(MAdMA$_{50}$-co-GBLMA$_{50}$); right: P(MAdMA$_{41}$-co-GBLMA$_{59}$).
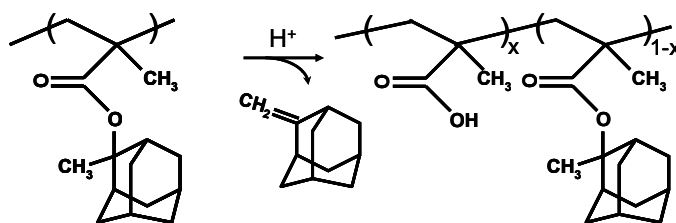
Scheme 2. Acid catalyzed deprotection of PMAdMA.

Table I. Polymer characteristics of the three photoresists

Polymer	M_w	M_w/M_n	Glass Transition Temperature
PMAdMA	8,800	1.18	> 210 °C
P(MAdMA$_{50}$-co-GBLMA$_{50}$)	12,800	1.67	161.9 °C
P(MAdMA$_{41}$-co-GBLMA$_{59}$)	11,505	1.3	171.5 °C

2. Sample preparation

Double-side polished, N-doped, high-resistivity silicon wafers with nominal thickness of 500 μm were obtained from Nova Electronic Materials, Texas. A solution containing a mixture of polymer and TPS-PFBS (19:1 by mass) in cyclohexanone solvent (5 % by mass) was spun coat on such wafers with a speed 209 rad/s (2000 rpm) at acceleration of 105 rad/s^2 (1000 rpm/s) for 60 s. The typical film thickness was approximately 150 nm as determined by x-ray reflectivity. The sample was post-apply baked at 130 °C for 60 s then exposed with a 248 nm broadband UV lamp. Different doses were produced by adjusting the exposure time on different areas of the wafer. The exposed samples were then transferred to a preheated hot-plate for post-exposure baking (PEB) immediately after exposure to minimize acid quenching by basic contaminants in the environment.[15]

[#] Certain commercial equipment and materials are identified in this paper in order to specify adequately the experimental procedure. In no case does such identification imply recommendations by the National Institute of Standards and Technology nor does it imply that the material or equipment identified is necessarily the best available for this purpose.

The effect of different copolymer compositions on acid diffusion was tested using a multiple layer scheme. Bilayer reference samples included an acid feeding layer and a detection layer. Trilayer samples include a layer between the acid feeding layer and detection layer.[16] The acid feeding layer consists of poly(4-hydroxystyrene) with 5% TPS-PFBS loading. The detection layer is the PMAdMA. The intermediate layer was poly(methacrylic acid) (PMAA) or PGBLMA. Bilayer and trilayer films are prepared utilizing the methods described earlier except with solvents chosen to ensure sharp interfaces between the layers.

3. FTIR spectroscopy

The deprotection reaction is measured with a Nicolet NEXUS 670 Fourier transform infrared (FTIR) spectrometer equipped with a liquid-nitrogen cooled MCT/A detector. The data are collected in transmission mode with the OMNIC online-data acquisition software. A resolution of 8 cm^{-1} is used and 128 scans are averaged to improve the signal-to-noise ratio. Samples after PEB are directly transferred to a N_2 gas purged FTIR chamber at room temperature. No significant change in the deprotection level or MA residual level is observed when the sample is stored at room temperature for five days and/or under continuous N_2 purge for 15 min.

The quantification of deprotection reaction degree is based on the bending vibration mode of CH_3 (1360 cm^{-1}) in the protecting MA group of PMAdMA, (Figure 1a). This band disappears completely and leaves a flat baseline in the IR spectra if all the protected MA groups are reacted. This band provides an absolute value of deprotection extent and allows for discrimination of free MA or residual MA from the protected MA group. For the copolymers, the CH_3 band is too weak to obtain high quality data. Instead, a C-O stretching band (1260 cm^{-1}) is used. (Figure 1b)

(a)   (b)
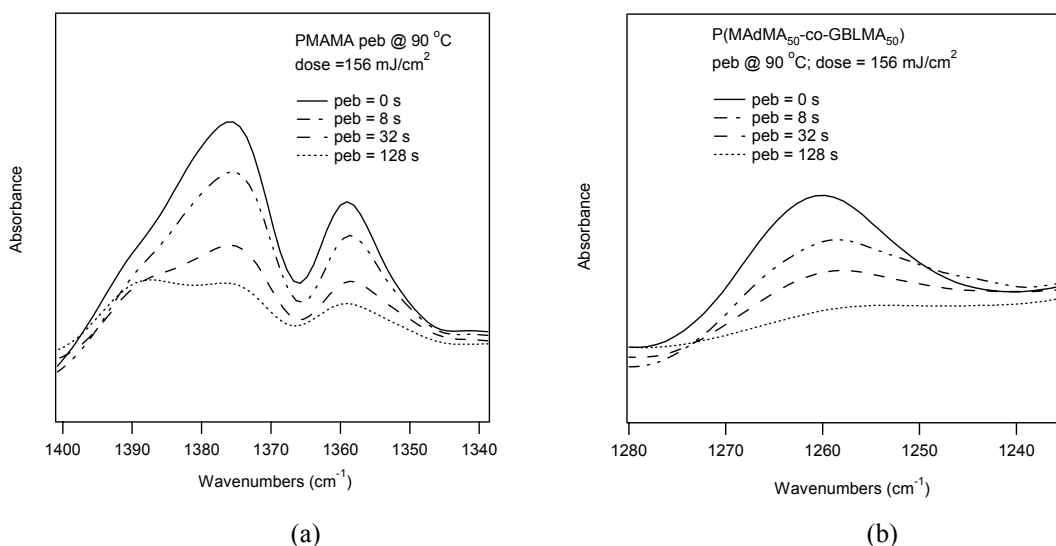
Figure 1. The spectroscopic bands used for the characterization of deprotection level in PMAdMA (a) and copolymers (b)

RESULTS AND DISCUSSION

Deprotection kinetics of three model photoresists

Figure 2a, 2b and 2c shows the time evolution of deprotection level for the photoresists at a PEB temperature of 110 °C containing 0 %, 50 % and 59 % mole GBLMA respectively. As expected, the deprotection level increases with dose and PEB time. For dose levels of 26 mJ/cm^2 and above, the deprotection level is similar, suggesting complete photolysis of the PAG. However, the deprotection level reaches a plateau at lower or intermediate doses, implying that the deprotection reaction has almost stopped. By comparing the deprotection level at a given dose and PEB time between different resists, we find that the deprotection rate decreases with an increase in GBLMA comonomer content.
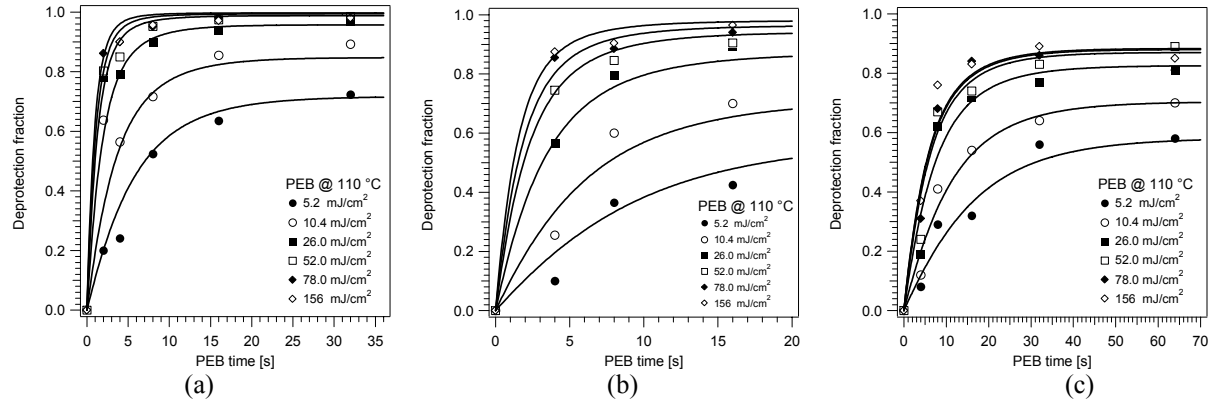
Figure 2. The absolute molar deprotection level versus post-exposure bake time for the resist copolymers : (a) PMAdMA, (b) P(MAdMA$_{50}$-co-GBLMA$_{50}$), (c) P(MAdMA$_{41}$-co-GBLMA$_{59}$) containing 5.0 % by mass TPS-PFBS photoacid generator. The dose is provided in the legend. The continuous lines are fits to the chemical reaction kinetics model discussed in the text.

Acid catalyzed reaction model

The deprotection process includes photoacid generation, photoacid diffusion, a catalyzed reaction with acid labile moieties, and the removal of methylene adamantane. A model is needed to quantify the reaction kinetics as a function of exposure dose, PAG loading, and other factors such as byproducts and comonomer composition.

Here, we develop a model that first describes the UV exposure step that initiates the photoacid generator, followed by the reaction step at elevated temperature leading to deprotection of the acid-labile groups. The concentration of photoacid can be calculated from the exposure dose by the following,

$$[H+] = [PAG]_0 \, [1\text{-}\exp(-C\,E)]. \tag{1}$$

The [H+] and [PAG]$_0$ are the photoinitiated and initial PAG concentrations, respectively, E is the exposure dose and C is the Dill parameter that quantifies the efficiency of photolysis. The mechanism of the dissociation and subsequent diffusion of the acid is not simple considering it is an electrolyte species. There are varied descriptions of the acid diffusion process [10-13,16-18]. The photoacid can be viewed as completely dissociated and diffuses as free ions in the polymer matrix. However, it has been shown that the size of photoacid counter-anions affect the diffusivity[13]. Therefore, we assume the acid diffuses cooperatively as a single species with its conjugate base counter-anion[13,17]. This assumption is appropriate for strong acids, such as perfluorobutanesulfonic acid. However, weaker acids are less dissociated in weakly polar or even non-polar polymer matrices[19].

The acid catalyzed reaction includes both diffusive and reactive processes. As the reaction proceeds, protected groups are cleaved leading to a methacrylic acid (MAA) product as governed by the chemical equation (2). An auto-acceleration effect by reaction products, reported for a hydroxystyrene system [19] was not observed in these experiments, nor from results from Paniez et al. [20], which uses a similar methacrylate system.

$$[MAdMA] + [H+] \rightarrow [MAA] + [MA] + [H+] \tag{2}$$
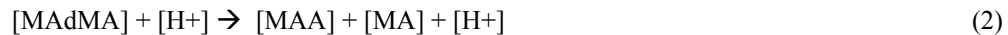
The evolving polymer matrix can influence the mobility of the photoacid. The photoacid diffusion coefficient can vary by several orders in magnitude between the protected versus deprotected polymer [16]. This appears as a reduced reaction rate in the presence of the deprotected polymer when the reaction is diffusion controlled [21]. However, it is challenging to model a variable diffusivity because the system must be treated heterogeneously such as in mesoscale simulation methods of Schmid et al.,[22] or in stochastic simulation methods of Houle et al.. [11] An alternative approach is to assume that the system is homogeneous, i.e. the gradient of acid concentration is zero, but the photoacid can be effectively trapped by MAA, implying the diffusion coefficient becomes very small in MAA-rich regions as shown in Equation 3. This assumption is verified as will be discussed in greater detail.

$$[H+] + [MAA] \rightarrow [H\text{-}MAA]_{Trapped} \tag{3}$$

A relationship was obtained by solving the two differential equations based on the above chemical reaction equations,

$$d[MAdMA]/dt = -k_P [H+] [MAdMA] \tag{4}$$
$$d[H+]/dt = -k_T [MAA] [H+] \tag{5}$$

where [MAdMA], [MAA], [H+] are the molar concentration of MAdMA, MAA, and the photoacid. For convenience, we use relative concentrations for MAdMA and MAA which are defined as their concentration at time t relative to the initial MAdMA concentration, $[MAdMA]_0$. Since this is a time-independent constant, its insertion does not affect the above equations. The k_P and k_T are the acid catalysis reaction constant and trapping rate constant for the acid, respectively. Many investigations assume the acid catalyzed reaction rate follows first order kinetics in concentration of acid and reactant[19,21,23]. Zuniga et al. found that non-first order reaction kinetics can be used to explain a nonlinear behavior of feature critical dimension with dose. [14,24] Despite the variety of modeling, it is generally agreed that the use of first order kinetics alone is too simple to describe the kinetics completely, especially at later reaction stage when the deprotection level is high.

The deprotection level (ϕ) can be calculated from the relative molar concentration of MAdMA groups.

$$\phi \equiv 1 - [MAdMA]/[MAdMA]_0 = [MAA]/[MAdMA]_0 \tag{6}$$

Rearranging the above equations and solving for [H+], results in the following expression:

$$[H+] = [H+]_0 + k_T/k_P [MAdMA]_0 [\phi + \ln(1-\phi)] \tag{7}$$

$$d\phi/dt = k_P [H+] (1-\phi) \tag{8}$$

where $[H+]_0$ is the initial photoacid concentration determined by equation (1). The deprotection level is calculated by combining equation (1), (7) and (8). Therefore by fitting these equations to the data, we can determine Dill's parameter (C), the reaction constant (k_P) and acid trapping factor (k_T). Since several dose values were measured our approach provides independent verification of the reaction rate constants and increases confidence in the results. A MatLab computer program was used to fit the experimental data to the model using a least-squares regression routine. The deprotection level defined also applies to copolymers because only the MAdMA functional groups take part in the reaction. The initial number density of MAdMA requires adjustment to account for the comonomer dilution as summarized in Table II. All the fitting parameters for the three photoresists examined are listed in Table III.

Table II. Resist compositional characteristics

Polymer Resists	Mass fraction of MAdMA (ε)	Density (ρ)[a] (g cm^{-3})	$[PAG]_0$ (nm^{-3})[b]	$[MAdMA]_0$ (nm^{-3}) [c]
P(MAdMA)	1	1.13	0.061	2.86
P(MAdMA$_{50}$-co-GBLMA$_{50}$)	0.577	1.20	0.065	1.75
P(MAdMA$_{41}$-co-GBLMA$_{59}$)	0.487	1.23	0.067	1.52

[a] The film density values were determined by X-ray reflectivity

[b] $[PAG]_0 = 0.05 \rho N_A / M_{o,PAG}$

[c] $[MAdMA]_0 = \varepsilon \rho N_A / M_{o,MAdMA}$

ρ is the mass density of polymer resists, M_o is the repeat unit molar mass, ε is the mass fraction of MAdMA in a polymer chain and N_A is the Avogadro's constant.

Table III: Summary of reaction kinetics parameters*

Experiments	Temp.	C (cm^2/mJ)	k_P (nm^{3}s^{-1})	k_T (nm^{3}s^{-1})
P(MAdMA)	110 ^{o}C	0.022 ± 0.003	17.4 ± 0.7	0.073 ± 0.011
P(MAdMA$_{50}$-co-GBLMA$_{50}$)	110 ^{o}C	0.018 ± 0.006	9.7 ± 1.0	0.114 ± 0.037
P(MAdMA$_{41}$-co-GBLMA$_{59}$)	110 ^{o}C	0.050 ± 0.013	2.0 ± 0.2	0.100 ± 0.014

* The standard uncertainty ($\pm$) for all the parameters are corresponding to one standard deviation obtained by fitting the kinetics data with regression model.

Acid catalyzed reaction rate

As the GBLMA content increases the apparent reaction rate constant, k_P, decreases as shown in Figure 3. Under an ideal fully-mixed chemical reaction condition or when the mobility of reactant molecules is high relative to the reaction rate, the rate constants should be independent of the reactant concentrations. However, the apparent rate constant for this system includes the effects of photoacid strength, diffusivity[21] and resist polarity[25]. Since the photoacid strength is fixed, the trends in the reaction constants are attributed to the polarity of the thin film and the resulting acid diffusivity. The interaction of the polymer with the photoacid is enhanced by substituting the non-polar MAdMA group with the polar GBLMA one. The carbonyl group of GBLMA and the acrylate on the main chain can hydrogen bond with the photoacid (unpublished FTIR results). This was observed by Lee et al.[26] as model probe diffusion coefficients were greatly reduced by hydrogen bonding interactions with a polymer in solution.
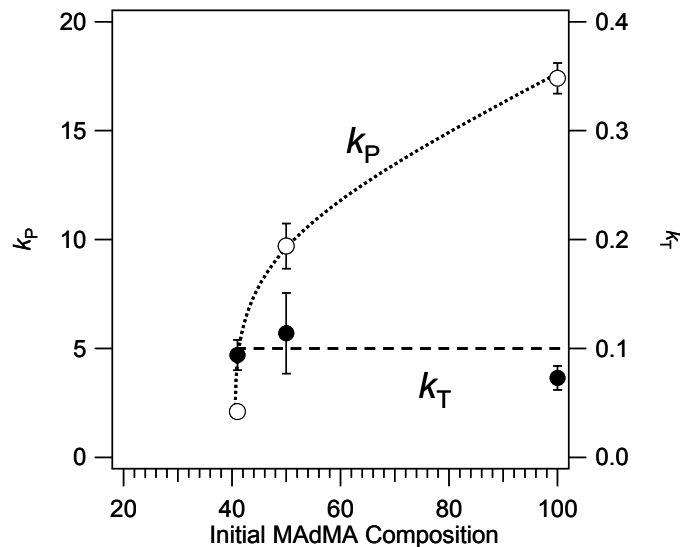
Figure 3. Summary of the rate constants for acid catalysis (k_P) and apparent acid trapping (k_T) as a function of the methyladamantyl protecting group content at PEB temperature of 110°C. The lines are drawn for guiding the eye.

In order to identify how the GBLMA comonomer interacts with the photoacid, we followed the procedure developed by Postnikov[16] using a bilayer and trilayer experiment. In our case, the detection layer should be sensitive enough such that the reaction is immediately detected once the photoacid diffusion front arrives. Using an acid feeder layer in direct contact with PMAdMA it only takes 8 s to 15 s for (50 to 70) % mol deprotection to occur[27]. In this case, there is no barrier for the acid to diffuse. When an intermediate layer of PGBLMA is used in the trilayer case, 120 s to 240 s is required to achieve similar deprotection levels at identical reaction conditions. In this case, the film thickness of the intermediate layer is comparable with the detection layer, so the diffusion coefficient of photoacid in PGBLMA is estimated to be approximately one order of magnitude (8 $\times$ to 30 $\times$) smaller than that through PMAdMA. Thus, the diffusivity of photoacid is reduced by the GBLMA content. The subsequent molecular mechanism of how a local composition fluctuation in GBLMA influences the trajectory of the photoacid can only be captured through inhomogeneous modeling[28].

A quantitative relationship between photoacid diffusivity and the apparent reaction constant was proposed by Nakamura et al.[29]. They proposed that the observed reaction rate constant is proportional to the diffusion coefficient of photoacid and resist reaction probability per photoacid. For the case of fixed acid cleavable group

chemistry, the reaction probability will be independent of comonomer content. Therefore our observed reduced k_P with increased GBLMA content is consistent with a reduced photoacid diffusivity.

Acid self-quenching

As the reaction proceeds and the deprotection products increase in local concentration, the reaction slows down. This effect could be interpreted through an acid loss factor[14,23,24], or varied diffusion coefficient[13], or even changing reaction order[24]. We eliminated the likelihood of a changing reaction order. The data will be shown in a future publication. The results for the acid-trapping or self-quenching rate constant (k_T) are summarized in Table III and plotted in Figure 3. This quenching rate constant is independent of the initial copolymer fraction. Therefore, it arises from a source fundamentally different than the reduced reaction rate constant due to the non-reactive lactone comonomer.   It is also differentiated from a typical loss factor which is only linear in photoacid concentration and independent of resist composition[14]. The photoacid may appear inactive through such a reduced diffusivity and only occurs as the deprotection products increase in local concentration through a proposed first-order reaction (Eq. 3).

To demonstrate the reduced diffusivity of the photoacid, we again use a trilayer experiment with poly(methacrylic acid) as the intermediate layer. Following the same exposure and bake conditions as the GBLMA study, no deprotection reaction was detected after 1 h. Therefore, in comparison the diffusion of photoacid in poly(methacrylic acid) or methacrylic acid rich regions is expected very slow when compared with protected resists over the time scale of a typical reaction (less than 3 min). It is not clear how many methacrylic acid units are necessary to trap one photoacid. However, the first-order reaction in MAA and photoacid with k_T characterizing the trapping is sufficient in this model.

The diffusion of small-molecules in polymers below the glass transition temperature is a topic that has been investigated in detail and the reaction temperatures used here are well below the polymer glass transition. In this system, the free volume is expected to be relatively independent of polymer type and is approximately constant. [30] The trend of the apparent reaction rate constants is counter to that expected from differences in the glass transition temperature of the polymers. For instance, the PMAdMA has a higher glass transition than the copolymers as shown in Table I, yet the reaction rate is a factor of 8.7 larger for the PMAdMA than P(MAdMA$_{41}$-co-GBLMA$_{59}$) from Table III.

CONCLUSIONS

The deprotection reaction kinetics in model 193 nm photoresists are influenced by the comonomer composition and reaction products. A simple chemical reaction kinetics model describes the dependence of the deprotection level on reaction time and photoacid concentration. Through this model, the deprotection reaction rate constant decreases with increased lactone content. This is attributed to a systematic decrease of photoacid transport due to hydrogen bonding with the polar groups in the gamma-butyrolactone functional groups. Similarly, an expression to understand the slowing down of the reaction at high extent of reaction is explained by hydrogen bonding between photoacid and the methacrylic acid groups. These observed relationships between the deprotection reaction kinetics and the polymer microstructure highlight additional competing processes that must be included in future reaction-diffusion experimentation and modeling.

ACKNOWLEDGEMENTS

References

1. Ito, H. Chemical amplification resists for microlithography. *Adv. Polym Sci.* **2005,** *172*, 37-245.

2. Wallraff, G.; Hinsberg, W. D. Lithographic imaging techniques for the formation of nanoscopic features. *Chem. Rev.* **1999,** *99*, 1801-1821.

3. Berger, C. M.; Henderson, C. L. Improved method for measuring photoacid generator kinetics in polymer thin films using normalized interdigitated electrode capacitance data. *Journal of Vacuum Science & Technology B* **2004,** *22* (3), 1163-1173.

4. Berger, C. M.; Byers, J.; Henderson, C. L. Using interdigitated electrodes for measuring photoacid generator kinetics in chemically amplified resists. *Journal of Electrochemical Society* **2004,** *151* (2), G119-G130.

5. Feke, G. D.; Hessman, D.; Grober, R. D.; Lu, B.; Taylor, J. W. On-wafer spectrofluorometric evaluation of the response of photoacid generator compounds in chemically amplified photoresists. *Journal of Vacuum Science & Technology B* **2000,** *18* (1), 136-139.

6. Pawloski, A. R.; Nealey, P. F. Effect of photoacid generator concentration on sensitivity, photoacid generation, and deprotection of chemically amplified resists. *Journal of Vacuum Science & Technology B* **2002,** *20* (6), 2413-2420.

7. Shinozuka, T.; Tsunooka, M.; Itani, T.; Shirai, M. Activation energies for deprotection reaction of chemically amplified resists: A study using in-situ FT-IR spectroscopy. *Journal of Photopolymer Science and Technology* **2002,** *15*, 765-768.

8. Szmanda, C. R.; Brainard, R. L.; Mackevich, J. F.; Awaji, A.; Tanaka, T.; Yamada, Y.; Bohland, J.; Tedesco, S.; Dal'Zotto, B.; Bruenger, W.; Torkler, M.; Fallmann, W.; Loeschner, H.; Kaesmaier, R.; Nealey, P. M.; Pawloski, A. R. Measuring acid generation efficiency in chemically amplified resists with all three beams. *Journal of Vacuum Science & Technology B* **1999,** *17* (6), 3356-3361.

9. Tsiartas, P. C.; Schmid, G. M.; Johnson, H. F.; Stewart, M. D.; Willson, C. G. Quantifying acid generation efficiency for photoresist applications. *Journal of Vacuum Science & Technology B* **2005,** *23* (1), 224-228.

10. Berger, C. M.; Henderson, C. L. Improved chemically amplified photoresist characterization using interdigitated electrode sensors: Photoacid diffusivity measurements. *Proceedings of SPIE* **2004,** *5376*, 392-403.

11. Houle, F. A.; Hinsberg, W. D.; Morrison, M.; Sanchez, M. I.; Wallraff, G.; Larson, C.; Hoffnagle, J. Determination of coupled acid catalysis-diffusion processes in a positive-tone chemically amplified photoresist. *Journal of Vacuum Science & Technology B* **2000,** *18* (4), 1874-1885.

12. Itani, T.; Yoshino, H.; Fujimoto, M.; Kasama, K. Photoacid bulkiness on dissolution kinetics in chemically amplified deep ultraviolet resists. *Journal of Vacuum Science & Technology B* **1995,** *13* (6), 3026-3029.

13. Stewart, M. D.; Tran, H. V.; Schmid, G. M.; Stachowiak, T. B.; Becker, D. J.; Willson, C. G. Acid catalyst mobility in resist resins. *Journal of Vacuum Science & Technology B* **2002,** *20* (6), 2946-2952.

14. Nagahara, S.; Yuan, L.; Poppe, W. J.; Neureuther, A.; Kono, Y.; Sekiguchi, A.; Fujiwara, K.; Watanabe, T.; Taira, K.; Kusumoto, S.; Nkano, T.; Shimokawa, T. Understanding quencher mechanisms by considering photoacid-dissociation equilibrium in chemically-amplified resists. *Proceedings of SPIE* **2005,** *5753*.

15. Hinsberg, W. D.; Macdonald, S. A.; Clecak, N. J.; Snyder, C. D. Airborne Contamination of A Chemically Amplified Resist .2. Effect of Polymer Film Properties on Contamination Rate. *Chemistry of Materials* **1994,** *6* (4), 481-488.

16. Postnikov, S. V.; Stewart, M. D.; Tran, H. V.; Nierode, M. A.; Medeiros, D. R.; Cao, T.; Byers, J.; Webber, S. E.; Willson, C. G. Study of resolution limits due to intrinsic bias in chemically amplified photoresists. *Journal of Vacuum Science & Technology B* **1999,** *17* (6), 3335-3338.

17. Shi, X. Effect of coulomb interaction and pKa on acid diffusion in chemically amplified resists. *Journal of Vacuum Science & Technology B* **1999,** *17* (2), 350-354.

18. Nakamura, J.; Ban, H.; Tanaka, A. Effect of acid diffusion on performance in positive deep ultravoilet resists. *Journal of Vacuum Science & Technology B* **1992,** *12* (6), 3888-3894.

19. Wallraff, G.; Hutchinson, J.; Hinsberg, W. D.; Houle, F. A.; Seidel, P.; Johnson, R.; Oldham, W. Thermal and acid-catalyzed deprotection kinetics in candidate deep ultraviolet resist materials. *Journal of Vacuum Science & Technology B* **1994,** *12* (6), 3857-3862.

20. Paniez, P.; Gally, S.; Mortini, B.; Rosilo, C.; Sassoulas, P.-O.; Dammel, R. R.; Padmanaban, M.; Klauck-Jacobs, A.; Oberlander, J. Thermal phenomena in acrylic 193 nm resists. *Proceedings of the SPIE, Advances in Resist Technology and Processing XVI* **1999,** *3678*, 1352.

21. Nakamura, J.; Ban, H.; Tanaka, A. Influence of acid diffusion on the lithographic performance of chemically amplified resists. *Jpn. J. Appl. Phys*. **1992,** *31*, 4294-4300.

22. Schmid, G. M.; Stewart, M. D.; Singh, V. K.; Willson, C. G. Spatial distribution of reaction products in positive tone chemically amplified resists. *Journal of Vacuum Science & Technology B* **2002,** *20* (1), 185-190.

23. Krasnoperova, A. A.; Khan, M.; Rhyner, S.; Taylor, J. W.; Zhu, Y.; Cerrina, F. Modeling and simulations of positive chemically amplified photoresits for x-ray lithography. *Journal of Vacuum Science & Technology B* **1994,** *12* (6), 3900-3904.

24. Zuniga, M.; Neureuther, A. Reaction-diffusion modeling and simulations in positive deep ultraviolet resists. *Journal of Vacuum Science & Technology B* **1995,** *13* (6), 2957-2962.

25. Pohlers, G.; Barclay, G.; Stafford, C.; Barbieri, T.; Cameron, J. Why do weak acids not work in 193-nm photoresists? Matrix effects on acid catalyzed deprotection. *Proceedings of the SPIE, Advances in Resist Technology and Processing XXI* **2004,** *5376*, 79-93.

26. Lee, J.; Park, K.; Chang, T.; Jung, J. Polymer/probe interaction in probe diffusion through a polymer matrix. *Macromolecules* **1992,** *29*, 6977-6979.

27. Vogt, B. D.; Kang, S.; Prabhu, V. M.; Lin, E. K.; Satija, S. K.; Turnquest, K.; Wu, W. L. *SPIE* **2006**.

28. Houle, F.; Hinsberg, W. D.; Sanchez, M.; Wallraff, G.; Larson, C.; Hoffnagle, J. Determination of coupled acid catalysis-diffusion process in a positive-tone chemically amplified photoresist. *Journal of Vacuum Science and Technology B* **2000,** *18*, 1874-1885.

29. Nakamura, J.; Ban, H.; Tanaka, A. Influence of Acid Diffusion on the Lithographic Performance of Chemically Amplified Resists. *Japanese Journal of Applied Physics Part 1-Regular Papers Short Notes & Review Papers* **1992,** *31* (12B), 4294-4300.

30. Young, R. J.; Lovell, P. A. *Introduction to Polymers;* 2nd ed.; Stanley Thornes Ltd.: 1991.